A Biologically-Inspired Controller for Reaching Movements*

Micha Hersch and Aude G. Billard

LASA Laboratory, School of Engineering
EPFL
Station 9 - 1015 Lausanne - Switzerland
{micha.hersch, aude.billard}@epfl.ch

Abstract— **This paper presents a robotic arm controller for reaching motions. This controller applies two principles inspired by current theories of human reaching motions, namely the multi-referential control of movements and the dynamical system approach to biological control. The controller consists of a stable dynamical system active in a hybrid cartesian-joint angle frame of reference. Our results show that this controller has interesting properties in terms of stability and robustness to perturbations, and that its redundancy can be exploited for a simple solution to the joint limit avoidance problem.**

Index Terms— **dynamical systems control, multi-referential control, VITE, joint limit avoidance, DLS inverse**

I. INTRODUCTION

Despite numerous studies, the mechanisms underlying the control of goal-directed motion in biological systems are largely unknown. The large body of experimental results gathered over many decades of research has lead to a number of hypotheses and theories about the biological control of goal-directed motions. In this work, we present a robotic arm controller based on two principles underlying current theories of biological control. The first principle is multi-referential control, i.e., the idea that multiple frames of reference are jointly used for movement control. The second principle is the dynamical system control, i.e. the idea that movement control is mediated by a dynamical system, and that movement execution is obtained by varying the parameters or the input of this dynamical system.

Our controller illustrates the advantages of applying those principles for robot control. It both validates those principles and shows how bio-inspired approaches can lead to simple and attractive solutions to classical robotics problems (see [1] for another bio-inspired approach to reaching).

Dynamical system approaches have already been successfully applied to robot control in the case of mobile robots [2], humanoid robots [3] and robotic manipulators [4]. The work presented here differs from other works in

that it makes use of two concurrent dynamical systems acting on two different yet redundant representations of the movement. The resulting global system can thus exploit desirable properties of each of those representations and smoothly switch from one dynamical system to the other.

The rest of this paper is structured as follows. Section II recalls some experimental results and theories about the human control of reaching motions, among them the Vector Integration To Endpoint (VITE) model suggested by [5]. Our controller for reaching motion is then presented in section III. The implementation of the controller and some experimental results are described in sections IV and V respectively. Finally some conclusions are drawn in section VI.

II. HUMAN REACHING MOVEMENTS

A. Multi-referential control

In the eighties, a lot of work has been devoted to determining the frame of reference in which reaching movements were planned. Some studies [6]–[8] suggested that movements were planned according to constraints expressed in a cartesian body-centered frame of reference, while others [9], [10] suggested that movements were planned according to intrinsic constraints expressed in joint angle coordinates.
In the nineties, it became widely accepted that movements were not planned in a single frame of reference, but that many different frames of reference were involved in the planning and control of reaching motions [11]. In particular, a hybrid visuo-kinesthetic frame of reference was hypothesized in [12].

B. Dynamical systems

Traditionally, reaching has been (explicitly or implicitly) considered as a two-stage process. The first stage is the planning stage, which is followed by an execution stage. According to this view, a reaching trajectory is computed during the planning stage, and this trajectory is actually tracked during the execution stage. This is in line with the usual robotics applications, were the planner and the controller are two separate components.
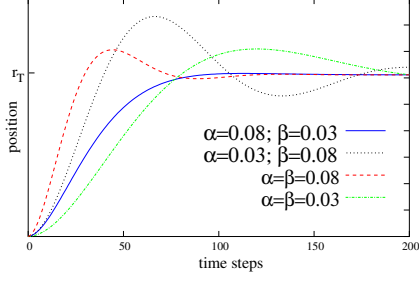
Fig. 1. The dynamics of the VITE model for various values of the parameters. Throughout this document the values $\alpha = 0.08$ and $\beta = 0.03$ were used. Refer to equation 3 for variable definitions.

Fig. 2. Global structure of the hybrid controller.

This traditional view has been challenged by the dynamical system approach to movement control [13]–[15]. According to this approach, there is no explicit trajectory planning, but rather an implicit set of trajectories made possible by a dynamical system. In this dynamical system, the target acts as an attractor for the arm. This view was supported by experimental evidence on frogs showing that an attractor could be created at a leg position by microstimulation of the spinal cord [16].

The exact nature of such a dynamical system is still controversial, although some suggestions have been made, such as Bullock's and Grossberg's Vector Integration To Endpoint (VITE) [5]. This model is described in the next paragraph.

1) The VITE model: The VITE model [5] describes the neural signals commanding a pair of agonist-antagonist muscles. The target limb position $\mathbf{T}$ is supposed to be known. The actual limb position is given by a signal $\mathbf{P(t)}$. The model hypothesizes the existence of a "difference vector population" of neurons with activity $\mathbf{V}$ and a "go signal" $G(t)$, which gates the execution of the movement. The VITE model for a single muscle is then described by the following equations:

$$\dot{\mathbf{V}} = \alpha(-\mathbf{V} + \mathbf{T} - \mathbf{P}) \qquad (1)$$
$$\dot{\mathbf{P}} = G[\mathbf{V}]^{+}, \qquad (2)$$

where α is a positive constant and $[\cdot]^{+}$ indicates the positive value function (i.e 0 if the argument is negative).

Applying this model on two muscles, agonist and antagonist, and taking a step-like go function yields

$$\ddot{\mathbf{r}} = \alpha(-\dot{\mathbf{r}} + \beta(\mathbf{r_T} - \mathbf{r})). \qquad (3)$$

In this equation, $\mathbf{r}$ represents the limb position under the influence of both agonist and antagonist muscles, $\mathbf{r_T}$ the target position and β is a constant between 0 and 1. The evolution of the position $\mathbf{r}$ given by this equation is illustrated in Fig. 1 for different parameters α and β.
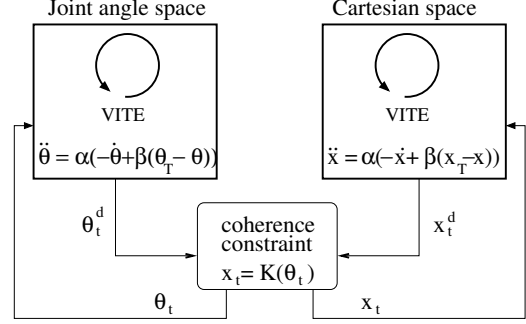
III. A BIOLOGICALLY-INSPIRED CONTROLLER FOR REACHING

A. Overview

The controller presented here is a simple implementation of the two principles described above, multi-referential control and dynamical system control. Basically, the controller can be summarized as a VITE dynamical system acting in a multi-referential space. This multi-referential space comprises the cartesian body-centered hand location space and the joint angle arm configuration space (see Fig. 2). In other words, there are actually two VITE dynamical systems, one in each of those spaces. Because a particular arm configuration corresponds to a particular end-effector location, those two spaces are not independent. Hence, coherence constraints between the two dynamical systems must be enforced in order to have a meaningful representation of the movement. A more formal and detailed description of the controller and the constraint enforcement mechanism is given in the next section.

B. Formal description

We consider a n-dof robotic manipulator acting in a m-dimensional workspace (in the present experiments $m = 3$, as we do not consider the end-effector orientation). The manipulator configuration is described by the values of all its joint angles, i.e., by a vector $\theta \in \Re^{\mathbf{n}}$. The end-effector location is denoted by a vector $\mathbf{x} \in \Re^{\mathbf{m}}$. Those vectors may be indexed by the time t, indicating that at that time the manipulator is in configuration $\theta_{\mathbf{t}}$ and the end-effector in location $\mathbf{x_t}$. The end-effector location $\mathbf{x}$ is related to the arm configuration θ by the relationship

$$\mathbf{x} = \mathbf{K}(\theta), \qquad (4)$$

where $\mathbf{K}$ is the kinematic function. Due to the redundancy of the manipulator, different values of θ may yield the same value $\mathbf{K}(\theta)$.

The aim of the controller is to smoothly bring the manipulator end-effector to a target location $\mathbf{x_T}$. To this location corresponds a set Θ_T of the manipulator's joint configurations.

As schematized in Fig. 2, the reaching model is made of two VITE controllers that operate in parallel. The first VITE controller operates in the cartesian endpoint location space, whereas the second VITE controller operates in the joint angle (or arm configuration) space. In order to make sure that at any time t, $\mathbf{x_t} = \mathbf{K}(\theta_\mathbf{t})$, coherence constraints between the two controllers must be enforced.

The hybrid reaching controller operates as follows. At time t, the target joint angle configuration $\theta_\mathbf{T}$ is chosen among the set Θ_T, so that it is the closest (in the Euclidean norm sense) to the actual configuration.

$$\theta_\mathbf{T} = \underset{\theta \in \Theta_\mathbf{T}}{\operatorname{argmin}} \|\theta - \theta_\mathbf{t}\|. \qquad (5)$$

Then, a desired manipulator configuration $\theta_\mathbf{t+1}^\mathbf{d}$ and end-effector position $\mathbf{x_{t+1}^d}$ are obtained independently by the two VITE controllers. This is done by applying equation 3 to the θ and $\mathbf{x}$ variables, which yields (using Euler approximation)

$$
\begin{align}
\dot{\theta}_\mathbf{t+1}^\mathbf{d} &= \dot{\theta}_\mathbf{t} + \alpha\big(-\dot{\theta}_\mathbf{t} + \beta(\theta_\mathbf{T} - \theta_\mathbf{t})\big) & (6)\\
\theta_\mathbf{t+1}^\mathbf{d} &= \theta_\mathbf{t} + \dot{\theta}_\mathbf{t+1}^\mathbf{d} & (7)\\
\dot{\mathbf{x}}_\mathbf{t+1}^\mathbf{d} &= \dot{\mathbf{x}}_\mathbf{t} + \alpha\big(-\dot{\mathbf{x}}_\mathbf{t} + \beta(\mathbf{x_T} - \mathbf{x_t})\big) & (8)\\
\mathbf{x_{t+1}^d} &= \mathbf{x_t} + \dot{\mathbf{x}}_\mathbf{t+1}^\mathbf{d}, & (9)
\end{align}
$$

where $\dot{\theta}_\mathbf{t} = \theta_\mathbf{t} - \theta_\mathbf{t-1}$ and $\dot{\mathbf{x}}_\mathbf{t} = \mathbf{x_t} - \mathbf{x_{t-1}}$. Usually, the desired arm configuration is incompatible with the desired hand location, i.e., $\mathbf{x_{t+1}^d} \neq \mathbf{K}(\theta_\mathbf{t+1}^\mathbf{d})$. Consequently, the system is brought to the position $(\theta_\mathbf{t+1}, \mathbf{x_{t+1}})$ which is closest to the desired position, while remaining compatible. This can be expressed by a constrained optimization problem and solved using the Lagrange multipliers technique:

$$
\begin{align}
\underset{\theta,\mathbf{x}}{\operatorname{Min}} \quad & (\theta - \theta^\mathbf{d})^\mathbf{T}\mathbf{W}^\theta(\theta - \theta^\mathbf{d}) + (\mathbf{x} - \mathbf{x^d})^\mathbf{T}\mathbf{W^x}(\mathbf{x} - \mathbf{x^d}) \\
\text{u.c.} \quad & \mathbf{x} = \mathbf{K}(\theta), & (10)
\end{align}
$$

where the time index $t+1$ has been dropped. In this formula the positive diagonal matrices $\mathbf{W}^\theta \in \Re^{\mathbf{n} \times \mathbf{n}}$ and $\mathbf{W^x} \in \Re^{\mathbf{m} \times \mathbf{m}}$ control the influence of each of the controllers. The solution to this optimization problem is given by:

$$
\begin{align}
\theta_\mathbf{t+1} = \ & \theta_\mathbf{t} + (\mathbf{W}^\theta + \mathbf{J_t^T W^x J_t})^{-1}\big(\mathbf{J_t^T W^x}(\mathbf{x_{t+1}^d} - \mathbf{x_t}) \\
& + \mathbf{W}^\theta(\theta_\mathbf{t+1}^\mathbf{d} - \theta_\mathbf{t})\big), & (11)
\end{align}
$$

where $\mathbf{J_t} \in \Re^{\mathbf{m} \times \mathbf{n}}$ is the Jacobian of the kinematic function $\mathbf{K}(\theta_\mathbf{t})$. By modifying the two parameters $\mathbf{W}^\theta$ and $\mathbf{W^x}$, one can vary the control strategy from a pure cartesian control ($\mathbf{W}^\theta = \mathbf{0}$) to a pure joint angle control ($\mathbf{W^x} = \mathbf{0}$). One can indeed notice, that after setting the $\mathbf{W}^\theta$ to zero and $\mathbf{W^x}$ to identity, the solution is equivalent to the classical Moore-Penrose pseudo-inverse solution presented in [17]. More interestingly, by setting $\theta_\mathbf{t+1}^\mathbf{d} = \theta_\mathbf{t}$ and $\mathbf{W}^\theta$ to identity, the Damped Least-Squares (DLS) inverse introduced in [18] to avoid singularities is obtained.

One way to understand the model is to see it as a VITE controller in the joint $(\mathbf{x}, \theta)$ space, whereby the current position is constantly projected on the manifold described by equation 4. As such it is a linear dynamical system projected on a derivable nonlinear manifold.

C. Joint limit avoidance

When controlling a robotic arm, it is important to avoid the robot joint limits. Indeed, beside damaging the robot, running into a joint limit produces jerky movements and may bring the robot into dead-end states, from which it can then be difficult to escape. Many solutions to the joint limit avoidance problem have been suggested, such as the Gradient Projection Method [19] or the Weighted Least-Norm Solution [20]. Those generally consist of minimizing a penalty function that will attract the robot to the workspace center.

Here we show how we can exploit the topology of the multi-referential controller in order to design a simple and elegant solution to the joint avoidance problem.

This solution is based on the observation that the working space is convex when expressed in joint angle coordinates. Indeed, the working space is specified by independent maximum and minimum values for each dof, which makes the working space a hyper-parallelepiped when expressed in joint angle coordinates. Because this is a convex hyper-volume, any two points within the workspace can be joined by a straight segment contained in the workspace. Thus, a joint angle VITE controller, which produces straight trajectories, will never bump into the workspace boundaries. By contrast, a cartesian VITE controller may well bring the robot to its joint limits because the cartesian workspace is not convex.

Consequently, joint limits can be avoided by gradually moving to a joint angle control when approaching the workspace boundaries. This can be achieved by making the weights dependent on the arm configuration as follows:

$$\frac{w_t^x}{w_t^{\theta^i}} = \frac{1}{2}\gamma\Big(1 - \cos\big(2\pi\frac{\theta_t^i - \theta_{min}^i}{\theta_{max}^i - \theta_{min}^i}\big)\Big), \qquad (12)$$

where w_t^x is the cartesian weight (i.e., a diagonal element of W^x), $w_t^{\theta^i}$ is the weight of angle i at a given time t (i.e., a diagonal element of W^θ), θ_{min}^i and θ_{max}^i are the corresponding joint angle boundaries, θ_t^i is the corresponding angular position at time t and γ is a constant setting the maximum value for w^x/w^{θ^i}. The right-hand side of this equation is plotted on Fig. 3, left. By applying this formula, the control is purely angular ($w^x = 0$) when the system is approaching the joint boundary, thus avoiding it.

IV. IMPLEMENTATION

The model was validated to control the arms of a Hoap2 humanoid robot from Fujitsu we have in our lab. This robot has a four dofs arm, which makes it a redundant manipulator, as we discard the end-effector orientation. Of course, the controller described above is not restricted to
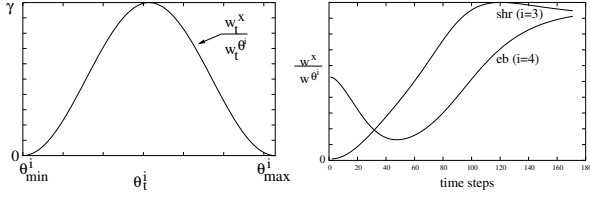
Fig. 3. Left: The value of the weight ratio depending on the manipulator configuration, see equation 12 and below for symbol definitions. Right: An example of the evolution of this ratio over time, for the movement described in Fig. 6.
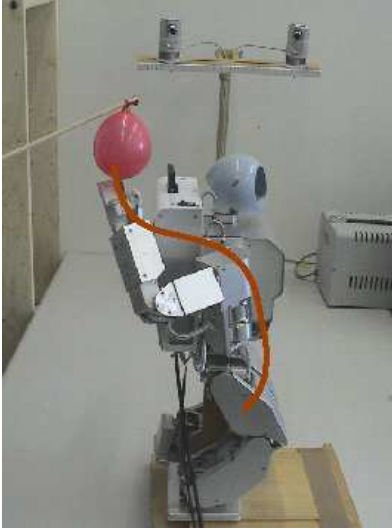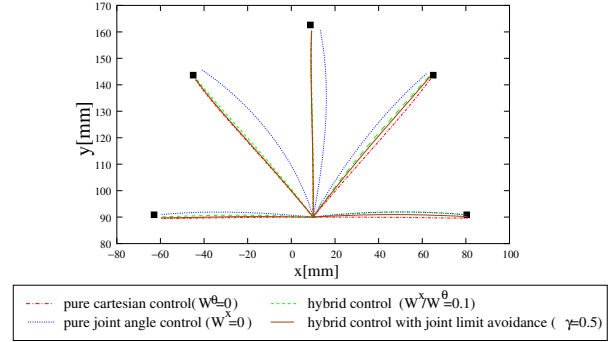

Fig. 5. Reaching trajectories for various weight configurations. The trajectories lie in the center of the workspace.
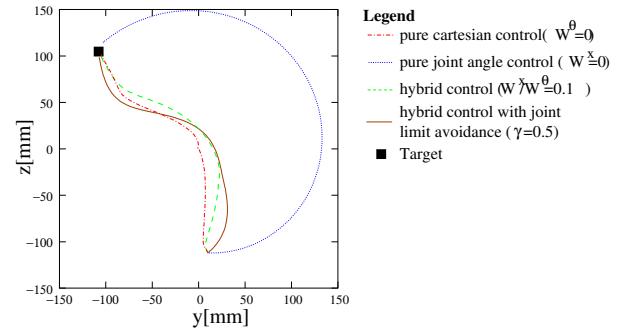

Fig. 6. End-effector trajectories for a movement nearby the workspace boundaries. The various trajectories illustrate the effect of the weights. Fig. 4 shows the corresponding end robot position.

Fig. 4. The robot reaches for the target tracked by a stereovision system. The line illustrates the end-effector trajectory.

such arms. It can control any kind of serial manipulator. In our setting, an external stereovision system endowed with a color detection module continuously tracks the target (here a red balloon). The cartesian location of this target is then given to the hybrid controller which controls the robot in position via a Realtime Linux platform. Fig. 4 shows the robot reaching for the target and the stereovision system.

V. RESULTS

A. Point-to-point reaching

The controller can perform accurate point-to-point reaching motions. Fig. 5 shows the reaching trajectories for movements in the workspace center using either a pure cartesian, a pure joint angle controller, a hybrid, or a joint limit avoidance hybrid controller. Like in human reaching motions, the trajectories resulting from the hybrid controllers are quasi-straight.

B. Joint limit avoidance

The joint limit avoidance method described above is tested on a reaching movement nearby the workspace boundaries; the robot is reaching behind its neck as in Fig. 4. The resulting end-effector trajectories are displayed on

Fig. 6 and two of the joint angle trajectories are shown in Fig. 7. As expected, the pure cartesian controller and the simple multi-referential controller cannot avoid the robot joint limit, which results in discontinuities in the joint angle velocity and sharp acceleration peaks. In contrast, the pure joint angle and the joint limit avoiding hybrid controllers effectively avoid the joint boundaries, which results in smoother movements. The latter controller produces shorter end-effector trajectories and is thus better. Indeed, the joint avoiding hybrid controller produces trajectories with the smallest hand path squared jerk $G = \int_{x_0}^{x_T} \|\dddot{x}\|^2 dx$ for any weight ratio (see Fig. 8). The jerk is a classical trajectory measure which penalizes unsmooth and long trajectories. It has been suggested that human reaching movements minimize this quantity [21].

C. Robustness to perturbations

As already shown in [5], the VITE equation forms a stable attractor at the target location. Therefore, the controller presented here reaches the target despite possible perturbations. This is illustrated in Fig. 9, which shows how the system adapts its trajectory in the face of sudden target displacements. The trajectory remains smooth, and the velocities remain continuous. This is guaranteed by the fact that the VITE system is a second-order linear system.
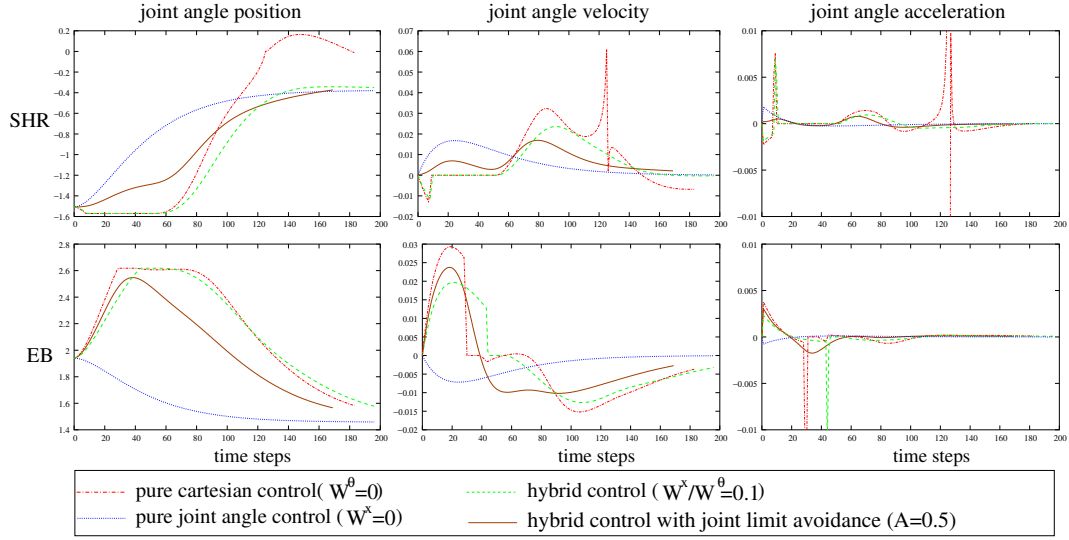
Fig. 7. The joint angle trajectories for two joints (SHR and EB) corresponding to the trajectory shown in Fig. 6.
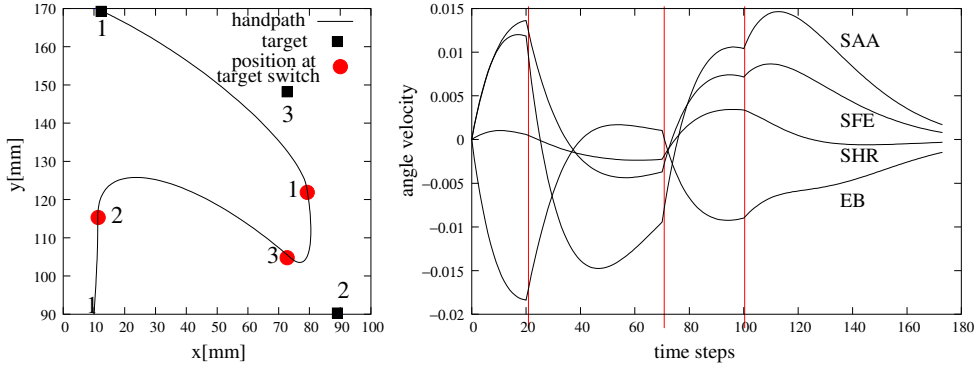

Fig. 9. The effect of a sudden target displacement on the trajectory. Left: the system starts reaching for target 1. When the system is at the locations indicated by the circles, the target is switched to the square with the corresponding number. One sees that the system smoothly adapts its trajectory to reach the new target. Right: The joint angle velocities corresponding to the trajectory depicted on the left. The vertical bars indicate the occurrences of target switching. SFE, SAA, SHR, EB correspond to the four dofs of our robotic arm.
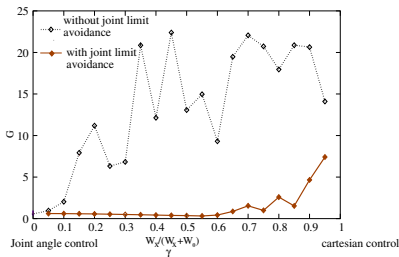

Fig. 8. The integral of the squared jerk G for the task Fig. 6 for various parameters. The abscissa represents the influence of the cartesian controller. The joint limit avoiding controller produces smoother trajectories.

VI. DISCUSSION

In the preceding sections, we described a robotic manipulator controller based on two basic principles drawn from the studies of human reaching movements, multi-referential movement representation and dynamical system control. The controller comprises two VITE dynamical systems, one acting on the end-effector described in a body-centered cartesian frame of reference and the other acting on the joint angle arm configuration. The controller is interesting both for robotics and for biological control modeling.

A. Strength of the controller

From a pure roboticist perspective, the multi-referential controller presented here has several advantages over classical controllers. First, it does not have any singularity because it uses a generalized version of the DLS inverse which has been shown to avoid the singularity problem [18]. Indeed, it is trivial to show that the inverse in equation 11 can always be computed as long as $\mathbf{W}^\theta$ is positive definite.

Another advantage of the controller is that it allows a simple and elegant solution to joint limit avoidance prob-

lem. Our results show that this method is effective and yields smooth and short end-effector trajectories. Note that this method makes the assumption that the joint angle workspace is convex, which is generally the case in the absence of obstacles.

Finally, the controller is robust to unexpected changes in the target location and smoothly adapts its trajectory accordingly. This is due to the robustness of the dynamical system underlying the controller.

B. Biological inspiration

This robotic controller is biologically inspired in the sense that it tries to apply some of the putative basic principles of biological control to a robotic arm. More precisely, the movement is specified by a dynamical system acting in a multi-referential space. Those two principles, dynamical systems and multi-referential control, have been argued to be essential to the human control of reaching movement [11], [14]. Those are the main biologically-inspired properties of our controller. In addition to those two properties, the VITE dynamical system and the frames of reference used by the controller have some biological plausibility. However it is *not* our claim that biological control of reaching motions uses this particular dynamical system acting on those particular variables and, *a fortiori*, not that it optimizes equation 10. The claimed analogy to biological systems lies in the general structure, not in the precise implementation. Hence, we do not expect a quantitative similarity between the controller-generated movements and human movements, but rather a qualitative similarity due to the same underlying principles. This qualitative similarity seems quite difficult to assess. Nonetheless, the controller-generated movements do have some common properties with human movements, either due to the VITE model such as the speed-accuracy trade-off and the speed-to-distance proportionality, or due to the multi-referential control such as being "a compromise between a straight line in workspace and a straight line in joint space" [22].

C. Conclusion

The idea of concurrent dynamical systems (or controllers) interacting with each other and leading to the emergence of a global behavior, is interesting for robot control as it provides robustness to failures of the individual controller and allows a smooth switching from one controller to the other, thus allowing multiple behaviors. It is also an appealing paradigm under which to study and model biological movement control, as it well suits the distributed computing performed in biological systems.

However, more research should be done to investigate under what conditions dynamical systems can be combined so that a global coherent behavior emerges. With the controller described in this paper, we have not observed deadlocks or unstable behavior. This can be intuitively understood by the fact that the dynamical systems have coherent attractors and

that the kinematic function is smooth. Nevertheless, more sophisticated tools are necessary to exploit the full potential of this approach.

REFERENCES

[1] A. Hauck, M. Sorg, G. Färber, and T. Schenk, "What can be learned from human reach-to-grasp movements for the design of robotics hand-eye systems?" in *Proceedings of the IEEE International Conference on Robotics and Automation*, 1999, pp. 2521–2526.

[2] G. Schöner, M. Dose, and C. Engels, "Dynamics of behaviour: theory and application for autonomous robot architecture," *Robotics and Autonomous Systems*, vol. 16, pp. 213–245, 1995.

[3] A. Ijspeert, J. Nakanishi, and S. Schaal, "Movement imitation with nonlinear dynamical systems in humanoid robots," in *Proceedings of the IEEE International Conference on Robotics and Automation*, 2002, pp. 1398–1403.

[4] I. Iossifidis and G. Schöner, "Autonomous reaching and obstacle avoidance with the anthropomorphic arm of a robotic assistant using the attractor dynamics approach," in *Proceedings of the IEEE International Conference on Robotics and Automation*, 2004, pp. 4295–4300.

[5] D. Bullock and S. Grossberg, "Neural dynamics of planned arm movements: Emergent invariants and speed-accuracy properties during trajectory formation," *Psychological Review*, 1988.

[6] P. Morasso, "Spatial control of arm movements," *Experimental Brain Research*, vol. 42, pp. 223–227, 1981.

[7] W. Abend, E. Bizzi, and P. Morasso, "Human arm trajectory formation," *Brain*, vol. 105, pp. 331–348, 1982.

[8] T. Flash and N. Hogan, "The coordination of arm movements: An experimentally confirmed mathematical model," *The Journal of Neuroscience*, vol. 5, no. 7, pp. 1688–1703, 1985.

[9] C. Atkeson and J. Hollerbach, "Kinematic features of unrestrained vertical arm movements," *The Journal of Neuroscience*, vol. 5, no. 9, pp. 2318–2330, 1985.

[10] F. Lacquaniti, J. Soechting, and S. Terzuolo, "Path constraints on point-to-point arm movements in three-dimensional space," *Neuroscience*, vol. 17, no. 2, pp. 313–324, 1986.

[11] J. Paillard, Ed., *Brain and Space*. Oxford University Press, 1991, chapters from Arbib, Berthoz and Paillard.

[12] M. Carrozzo and F. Lacquaniti, "A hybrid frame of reference for visuo-manual coordination," *Neuroreport*, vol. 5, pp. 453–456, 1994.

[13] E. Bizzi, N. Accornero, W. Chapple, and N. Hogan, "Posture control and trajectory formation during arm movement," *The Journal of Neuroscience*, vol. 4, pp. 2738–2744, 1984.

[14] J. Kelso, *Dynamic Patterns: The Self-Organization of Brain and Behavior*. MIT Press, 1995.

[15] E. Todorov and M. Jordan, "Optimal feedback control as a theory of motor coordination," *Nature Neuroscience*, vol. 5, no. 11, pp. 1226–1235, 2002.

[16] S. Giszter, F. Mussa-Ivaldi, and E. Bizzi, "Convergent force fields organized in the frog's spinal cord," *The Journal of Neuroscience*, vol. 13, no. 2, 1993.

[17] D. Whitney, "Resolved motion rate control of manipulators and human prosteses," *IEEE Transactions on Man-Machine Systems*, vol. 10, no. 2, 1969.

[18] C. Wampler, "Manipulator inverse kinematic solutions based on vector formulations and damped least-squares methods," *IEEE Transactions on Systems, Man, and Cybernetics*, vol. 16, no. 1, pp. 93–101, 1986.

[19] A. Liégois, "Automatic supervisory control of the configuration and behavior of multibody mechanisms," *IEEE Transactions on Systems, Man, and Cybernetics*, vol. 7, no. 12, pp. 868–871, 1977.

[20] T. F. Chan and R. Dubey, "A weighted least-norm solution based scheme for avoiding joint limits for redundant joint manipulator," in *Proceedings of the IEEE International Conference on Robotics and Automation*, 1995.

[21] N. Hogan, "An organizing principle for a class of voluntary arm movements," *Journal of Neuroscience*, vol. 4, pp. 2745–2754, 1984.

[22] H. Cruse and M. Brüwer, "The human arm as a redundant manipulator: The control of path and joint angles," *Biological Cybernetics*, vol. 57, pp. 137–144, 1987.